Is Weather Chaotic? Coexisting Chaotic and Non-chaotic Attractors Within Lorenz Models

Bo-Wen Shen, R. A. Pielke Sr., X. Zeng, J.-J. Baik, S. Faghih-Naini, J. Cui, R. Atlas, and T. A. L. Reyes

Abstract The pioneering study of Lorenz in 1963 and a follow-up presentation in 1972 changed our view on the predictability of weather by revealing the so-called butterfly effect, also known as chaos. Over 50 years since (Lorenz in J. Atmos. Sci. 20:130–141, [1]) study, the statement of "weather is chaotic" has been well accepted. Such a view turns our attention from regularity associated with Laplace's view of determinism to irregularity associated with chaos. Here, a refined statement is suggested based on recent advances in high-dimensional Lorenz models and real-world global models. In this study, we provide a report to: (1) Illustrate two kinds of attractor coexistence within Lorenz models (i.e., with the same model parameters but with different initial conditions). Each kind contains two of three attractors including point, chaotic, and periodic attractors corresponding to steady-state, chaotic, and limit cycle solutions, respectively. (2) Suggest that the entirety of weather possesses the dual nature of chaos and order associated with chaotic and non-chaotic processes, respectively. Specific weather systems may appear chaotic

B.-W. Shen (✉) · S. Faghih-Naini · J. Cui · T. A. L. Reyes
San Diego State University, San Diego, USA
e-mail: bshen@sdsu.edu

R. A. Pielke Sr.
CIRES and ATOC, University of Colorado At Boulder, Boulder, USA

X. Zeng
The University of Arizona, Tucson, USA

J.-J. Baik
Seoul National University, Seoul, South Korea

S. Faghih-Naini
University of Bayreuth, Bayreuth, Germany

Friedrich-Alexander University Erlangen-Nuremberg, Erlangen, Germany

J. Cui
North Carolina State University, Raleigh, USA

R. Atlas
University of Maryland, Baltimore County, Baltimore, USA

C. H. Skiadas et al. (eds.), *13th Chaotic Modeling and Simulation International Conference*, Springer Proceedings in Complexity,
https://doi.org/10.1007/978-3-030-70795-8_57

or non-chaotic within their finite lifetime. While chaotic systems contain a finite predictability, non-chaotic systems (e.g., dissipative processes) could have better predictability (e.g., up to their lifetime). The refined view on the dual nature of weather is neither too optimistic nor pessimistic as compared to the Laplacian view of deterministic unlimited predictability and the Lorenz view of deterministic chaos with finite predictability.

1 Introduction

Is weather chaotic? A view that weather is chaotic was proposed and is recognized based on the pioneering work of Lorenz [1] who first introduced the concept of deterministic chaos. Defined as aperiodic solutions that display sensitive dependence on initial conditions (ICs), chaos is also known as the butterfly effect. In a follow-up conference presentation in 1972 [2], the concept of sensitivity to ICs was further discussed by addressing whether a butterfly's flap may lead to a chain of responses that remotely generates a tornado. Since then, the butterfly effect has come to be known as a metaphor for indicating the huge impact of a tiny perturbation on the formation of a tornado. The original [1, 3] study and the 1972 presentation, as well as the 1969 study [4], laid the foundation for chaos theory that is viewed as the third scientific achievement in the twentieth century, after relativity and quantum mechanics, inspiring numerous studies in multiple fields, including earth science, mathematics, philosophy, physics, etc. [5].

While periodic solutions were a main focus until the [1] study, non-periodic solutions have increasingly received attention over the past 50 years. Lorenz's discovery has led to the statement of "weather is chaotic" and to a paradigm shift in the view of finite predictability from the Laplacian view of unlimited deterministic predictability. The idea of finite predictability for chaotic weather has prompted a search for the upper limit of predictability that was determined as 2 weeks based on analyses of unstable solutions from simplified models and data [4]. With the above being said, our current view on the chaotic nature of weather and a predictability limit of 2 weeks are based on the understanding of chaotic (as well as unstable) solutions obtained from elegant but simple models. To facilitate discussions, we define two kinds of predictability, including (1) intrinsic predictability that is dependent only on flow itself and (2) practical predictability that is limited by the imperfect initial conditions and/or (mathematical) formulas [6, 7].

Chaotic solutions are just one type of solution that occurs over finite intervals of time-independent parameters within the Lorenz model. To reveal the true nature of weather, we should take into consideration other types of solutions within original Lorenz models and newly developed generalized Lorenz models [7–24]. For example, in addition to chaotic solutions, two types of non-chaotic solutions indeed appear over different intervals of parameters within the Lorenz model [21]. Furthermore, recent studies using a generalized high-dimensional Lorenz model [16, 25–27] showed that chaotic and non-chaotic solutions may coexist within the same model

parameters but for different ICs [28, 29]. Thus, it is important to understand whether or not and how other types of solutions and their coexistence may help illustrate a more comprehensive view on the nature of weather, and to improve our understanding of predictability associated with different types of solutions. Specifically, we may ask whether the statement of "weather is chaotic" that exclusively considers chaotic solutions is scientifically precise.

To address the above, here, we first provide a review of major solutions using the Lorenz model (LM), including three types of solutions or three attractors in Sect. 2. In this study, a specific type of solution is referred to as an "attractor", defined as the smallest attracting point set that cannot be decomposed into two or more subsets with distinct regions of attraction [22]. We then summarize our recent findings for two kinds of attractor coexistence (i.e., with the same model parameters but with different initial conditions) using a newly developed, generalized, high-dimensional LM (GLM) [26] in Sect. 3. Section 4 is presented in order to support the findings for two kinds of attractor coexistence using the original LM with different parameters. Based on an analysis of the LM and the GLM and a brief review of previous studies (e.g., regarding 40-day intra-seasonal oscillations, coexisting solutions at two time scales, etc.), we suggest a refined view on the dual nature of weather in Sect. 5. Additional support for this view is also presented by the review of prior studies. Concluding remarks are provided in Sect. 6.

2 The Lorenz Model [1]

In his 1963 study, Prof. Lorenz presented an elegant system of three ordinary differential equations (ODEs) derived from the governing equations for the Rayleigh–Benard convection [1, 30]. The system describes the time evolution of three variables, X, Y, and Z, as follows:

$$\frac{dX}{d\tau} = \sigma Y - \sigma X, \tag{1}$$

$$\frac{dY}{d\tau} = -XZ + rX - Y, \tag{2}$$

$$\frac{dZ}{d\tau} = XY - bZ. \tag{3}$$

Here,τ is the dimensionless time. Three time-independent parameters include the Prandtl number (σ), the normalized Rayleigh number (r), also called the heating parameter, and a function of the ratio between the vertical and horizontal scales of the convection (b). (X, Y, Z) represent the amplitudes of the three Fourier modes for dynamic and thermodynamic variables. The system contains three types of physical processes, including buoyancy/heating terms (represented by σ Y and rX), dissipative

terms (represented by $-\sigma X$, $-Y$, and $-bZ$), and nonlinear processes (indicated by $-XZ$ and XY). With the exception of the heating parameter (r), the following parameters are kept constant: $\sigma = 10$ and $b = 8/3$. Control and parallel runs are performed in order to reveal the difference (or divergence) of two solutions. The only difference between control and parallel runs is that a parallel run includes tiny perturbations ($\in = 10^{-10}$) or finite perturbations ($\in = -0.9$) in initial conditions.

Using the state variables X, Y, and Z as coordinates, a phase space can be constructed for an analysis of solutions. An orbit or a trajectory is defined as the time varying components of solutions within the phase space. The dimension[1] of the phase space is equal to the number of time-dependent variables or to the number of ODEs. Thus, Eqs. (1), (2) and (3) with three variables are referred to as a three-dimensional Lorenz model (3DLM). High-dimensional LMs contain more than three variables.

2.1 Lorenz's Chaotic and Non-chaotic Attractors

Depending on the competitive or collective impact of nonlinear processes and linear buoyancy/heating and dissipative processes, various types of solutions (i.e., different attractors) appear within the Lorenz model. Historically, the dependence of their appearance on the strength of heating measured by the parameter (r) has been a focus. Steady-state, chaotic, and nonlinear oscillatory solutions have been shown to occur under conditions of weak, moderate, and strong heating, respectively [21, 33].[2] In Fig. 1, the three different types of solutions are shown using r = 20, 28, and 350, respectively. The top panels display solutions for control runs within the *X*-*Y* space, while bottom panels display the time evolution of the Y components for both control and parallel runs. For a steady-state solution, its orbit eventually approaches a single point, that is, a non-trivial equilibrium point within the *X*-*Y* space (Fig. 1a), appearing as a point attractor; and its amplitude remains constant over time after arriving at the equilibrium point. Mathematically, equilibrium points, also called critical points, are defined as solutions of the time-independent nonlinear system (e.g., no time derivatives in Eqs. (1), (2) and (3) [35].[3] When the heating parameter exceeds the critical value of $r_c = 24.74$, the 3DLM with r = 28 displays the so-called chaotic solution or a chaotic attractor with irregular oscillations. The solution's boundary within the *X*-*Y* space appears as a tilted "8" pattern. Interestingly, when heating becomes larger (e.g., r = 350), the system produces a nonlinear periodic solution known as a limit cycle solution or a periodic attractor, as shown in Fig. 1c and f.

[1] The term "dimension" is conventionally used for a system of ODEs [31, 32]. In this study, the 5DLM, 7DLM, and 9DLM are referred to as high-dimensional or high-order Lorenz models [12].

[2] Similar findings for the dependence of various solutions (i.e., chaotic and limit cycle solutions) on the strength of heating were also reported using a two-layer, quasi-geostrophic model that describes the finite-amplitude evolution of a single baroclinic wave by Pedlosky and Frenzen [34].

[3] In our 5D-, 7D-, and 9DLMs, we can obtain closed form solutions of trivial and non-trivial equilibrium points and use them to verify the numerical solutions of equilibrium points.

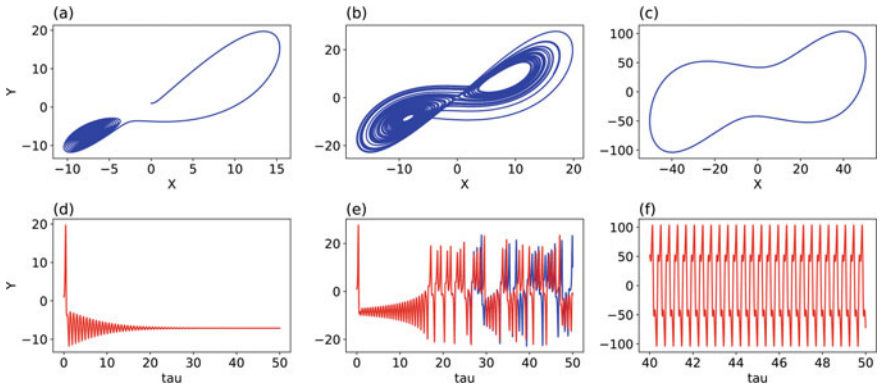

Fig. 1 Three types of solutions within the 3DLM. Left, middle, and right panels displays steady-state, chaotic, and limit cycle solutions at small, moderate, and large heating parameters (i.e., $r = 20$, 28, and 350), respectively. The solutions are categorized into a point attractor, a chaotic attractor, and a periodic attractor, respectively. Top panels show orbits within the X-Y space and bottom panels depict the time evolution of Y. Blue lines provide solutions from control runs. To display results from parallel runs, red lines are added in the bottom panels. Sensitive dependence on initial conditions is shown in panel (**e**) with two visible lines. Two panels, **b** and **e**, are reproduced from Shen [38]

Additional details on the characteristics of nonlinear oscillatory solutions may be found in earlier studies [21, 36, 37] and/or recent studies [16, 26, 38]. Below, the impact of a tiny initial perturbation on three attractors, including a point attractor, a chaotic attractor, and a periodic attractor, is further discussed.

Parallel runs with a tiny initial perturbation ($\in= 10^{-10}$) are compared to control runs in order to reveal the difference of initial, nearby trajectories within the phase space. For steady-state and nonlinear oscillatory solutions, control and parallel runs produce almost identical results, only appearing in red, for example, in Fig. 1d and f. The runs indicate insignificant impacts by a tiny initial perturbation. In other words, steady-state and nonlinear oscillatory solutions are insensitive to a tiny change in ICs. In comparison, within the chaotic regime, two solution orbits whose starting points are very close to each other display very different time evolutions, as clearly shown in blue and red in Fig. 1e. The phenomenon is called the sensitive dependence of solutions on ICs and only appears within a chaotic solution.

2.2 Boundedness and Divergence of Chaotic Trajectories

Within the chaotic regime, a sensitive dependence of solutions on ICs is referred to as the butterfly effect (BE, e.g., [39, 40]). As shown in Fig. 2a, the term "butterfly" was partly used due to its geometric pattern within the *Y*-*Z* space [39]. A butterfly pattern with a finite size and varying curvatures within the phase space also qualitatively suggests an important feature of solution boundedness. Therefore, BE means that a

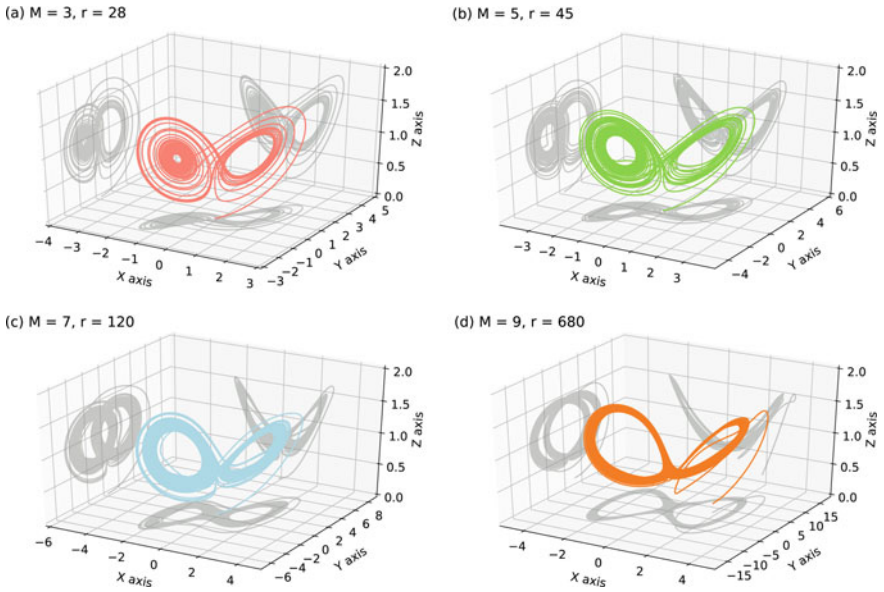

Fig. 2 Chaotic solutions in the X-Y-Z phase space within the 3D, 5D, 7D, and 9D Lorenz models (LMs). Panels **a**–**c** use the same initial conditions with Y = 1 and the remaining as zero, while panel **d** uses an IC with 100 for all variables. Variables (X, Y, Z) are normalized by $2\sqrt{r-1}$, $2\sqrt{r-1}$, and $(r-1)$, respectively. A larger heating parameter is required for the onset of chaos in a higher-dimensional LM. Also see the detailed analysis of solutions in Shen [38, 41]

tiny change in an IC can produce a very different time evolution of a solution for three variables (X, Y, Z). However, the separation (or divergence) of two orbits should be bounded by the size of a butterfly pattern.

The average separation rate (i.e., an average rate of divergence) of nearby trajectories has been quantitatively measured using the Lyapunov exponent (LE, [42–44]). A positive LE suggests an exponential rate in the averaged separation of two infinitesimally nearby trajectories over an infinite period of time (e.g., Eqs. (25) and (26) of [7]). Chaotic solutions within the 3DLM, as well as high-dimensional LMs, have a positive LE. Since the LE is defined as a long-term averaged separation, researchers often misinterpret the divergence of two nearby, but finitely separated, chaotic trajectories within the 3DLM as continuing over time and lasting forever. The misunderstanding also makes people believe that an unconstrained solution is due to the divergent nature of chaos [45]. In fact, in addition to a positive LE, solution boundedness is another major feature of a chaotic system. Due to solution boundedness, a trajectory should recurve within the phase space [45] Therefore, time-varying (local) growth rates along a chaotic orbit are observed [44] and may become negative, as indicated by a negative finite time LE [46–49]. In other words, the infinite-time limit in the definition of an LE does not imply a monotonically increasing separation between two nearby trajectories over a long period of time. Two initial nearby trajectories can quickly separate and reach the bound of their separation.

3 The Generalized Lorenz Model

The 3DLM produces three different attractors and each attractor exclusively appears within the phase space, depending on the interval of system parameters. The 3DLM with a single-type solution suggests that either chaos or order exclusively exists. By comparison, two different solutions may coexist and dominate system dynamics in a separate region (i.e., a different subspace) within the phase space within the same model, and with the same parameters, but with different ICs. Attractor coexistence has mainly been studied using conservative Hamiltonian systems [45], but can also be found in the forced dissipative 3DLM [33, 50, 51]. Below, we first discuss two kinds of attractor coexistence using the GLM, and then apply the GLM to understand whether the 3DLM can also possess two kinds of attractor coexistence.

Based on our recent studies [7, 26], we successfully developed a GLM that: (1) is derived based on partial differential equations for the Rayleigh–Benard convection;[4] (2) allows a large number of modes, say M modes, where M is an odd number greater than three; and (3) produces aggregated negative feedback[5] that is accumulated from the feedback of various smaller-scale processes, yielding a larger effective dissipation in higher dimensional LMs [26, 38]. *As a result of aggregated negative feedback, a higher-dimensional LM requires a larger critical value for the Rayleigh parameter (r_c) for the onset of chaos.* For example, the r_c for the 5DLM, 7DLM, and 9DLM are 42.9, 116.9, and 679.8, respectively, as compared to a r_c of 24.74 for the 3DLM [26]. Figure 2 displays chaotic solutions obtained from the 3D, 5D, 7D, and 9D LMs with different heating parameters. Therefore, an initial tiny perturbation with the same strength may play a different role within the GLM with a different value of M. Such a feature shows a dependence on the number of selected modes. Namely, it depends on the degree of spatial complexity associated with a various number of modes of the GLM.

3.1 Two Kinds of Attractor Coexistence

The GLM with M = 5 or M = 7 (i.e., 5DLM or 7DLM) also produces three different types of solutions, including a steady-state, chaotic, and limit cycle/torus.[6] More importantly, the GLM with M = 9 (i.e., 9DLM) displays two kinds of attractor coexistence, each with two different attractors. For the first kind of coexistence, both chaotic and steady-state solutions occur concurrently using the same model

[4] By comparison, chaotic models in Lorenz [52–54] were not derived from physics-based partial differential equations.

[5] Negative feedback can be found within the so-called Lorenz-Stenflo system that extends the 3DLM with one additional ODE containing one additional mode that takes rotation into consideration [55–57].

[6] A torus is defined as a composite motion with two (or more) oscillatory frequencies whose ratio is irrational [8].

and the same parameters. The only difference is their ICs. Such a coexistence shares properties similar to that of the 3DLM but appears over a wider range of the Rayleigh parameter (e.g., 679.8 < r < 1,058), as compared to the small interval (e.g., 24.06 < r < 24.74) for the 3DLM.

In addition to the first kind of attractor coexistence, the 9DLM is able to produce the second kind of attractor coexistence, consisting of nonlinear, periodic (i.e., limit cycle) orbits, and steady-state solutions at large Rayleigh parameters (e.g., r = 1,600). The new kind of coexistence was recently documented in Reyes and Shen [16], Shen [26] and Shen et al. [27]. Additionally, coexisting two periodic solutions were documented using the 9DLM with r = 1,120 [26]. As a result, when system parameters change at a large time scale (e.g., at climate time scales), different kinds of attractor coexistence may alternatively or concurrently appear, leading to complexities that better resemble real weather and climate.

3.2 Two Kinds of IC Dependence and Final State Sensitivity

Depending on system parameters, ICs and the dimension of the model (say the value of M within the GLM), a modeling system may contain one or more attractors[7] within the phase space. Since different attractors coexist, we expect different kinds of solution dependence on ICs, as illustrated using the 9DLM with r = 680 that produces the coexistence of chaotic and non-chaotic orbits. Control runs apply three sets of ICs at different locations within the phase space: close to the non-trivial equilibrium point, near the origin (i.e., a saddle point), and at point (100, 100, 100, 100, 100, 100, 100, 100, 100). For parallel runs, a finite-amplitude perturbation ($\in$ = -0.9) is added into the ICs. In Fig. 3, solutions of the control runs are shown in blue, while results of parallel runs are displayed in green, red, or orange. Top panels display the time evolution of the Y components, while bottom panels present solutions within the *X*-*Y* space. The model with r = 680 produces the coexistence of steady-state and chaotic orbits, displaying a dependence on ICs. For the first case (Fig. 3a and d) with the IC that is close to the non-trivial equilibrium point, the orbit moves toward the equilibrium point, producing steady-state solutions. Since the orbit spirals into the non-trivial equilibrium point within the *X*-*Y* space, it is also called a spiral sink solution. For the second case (Fig. 3b and e) where an IC is close to a saddle point at the origin but away from the non-trivial equilibrium point, solutions still approach the same non-trivial equilibrium point as a steady-state solution, while initially displaying a different time evolution as compared to the first case. On the other hand, for the third case (Fig. 3c and f), the model produces a chaotic solution, different from the steady-state solution. A comparison between control and parallel runs suggests that an initial perturbation only has a short-term impact on the initial

[7] The coexistence of chaotic and quasi-periodic orbits has been recently documented in a modified Lorenz system by Saiki et al. [58].

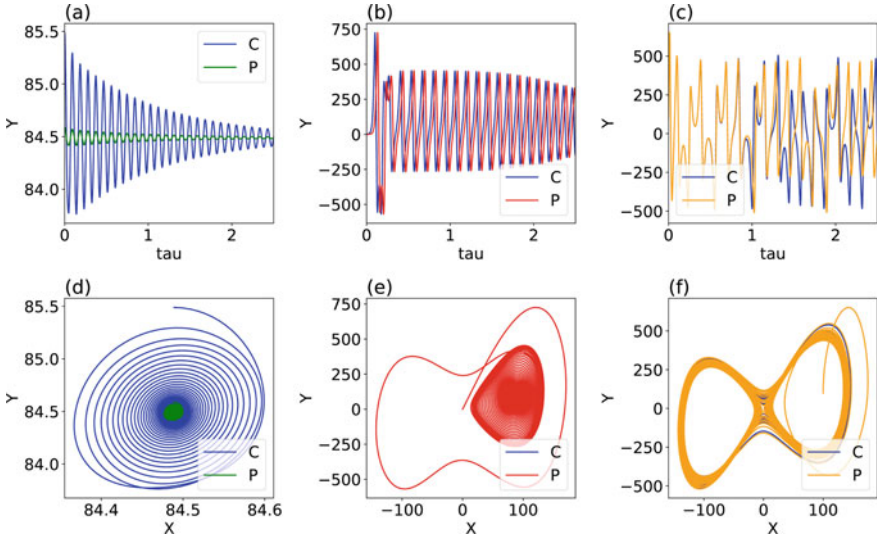

Fig. 3 Solutions of the GLM with M = 9 and r = 680. Initial conditions for the three cases are placed near the non-trivial critical point (**a**, **d**), the origin (i.e., trivial critical point) (**b**, **e**), and at (100, 100, 100, 100,100, 100, 100, 100,100) (**c**, **f**). Top panels show the time evolution of Y for $t \in [0, 2.5]$, while bottom panels display the corresponding solutions $t \in [0, 10]$ within the X-Y space. Control and parallel runs are denoted by 'C' and 'P', respectively. A finite-amplitude perturbation ($\in = -0.9$) is added into the parallel runs. Two panels, (**c**) and (**f**), are reproduced from Shen [38]

transient evolution of steady-state solutions but can lead to a very different evolution for chaotic solutions.[8]

When coexisting chaotic and regular attractors from 256 different initial conditions are plotted within the X-Y phase space, Fig. 4 clearly shows that chaotic and non-chaotic orbits occupy two different regions (or two different subspaces). Additional details on the spatial distribution of 256 initial conditions may be found in Shen et al. [27]. As a result of the different regions of attraction for coexisting attractors, final state sensitivity may appear [59] when ICs begin near the boundary of two different attractors. Such a sensitivity creates a different challenge for prediction.

3.3 Finite and Deterministic Predictability

The rate of a growing initial error with time has been used to determine predictability, suggesting a finite predictability in chaotic (or unstable) systems. Such a growth

[8] Such a dependence on initial conditions, close to (or away from) the non-trivial equilibrium point, can be shown by the following YouTube video for a double pendulum (between 1:00 and 1:20). https://www.youtube.com/watch?v=LfgA2Auyo1A.

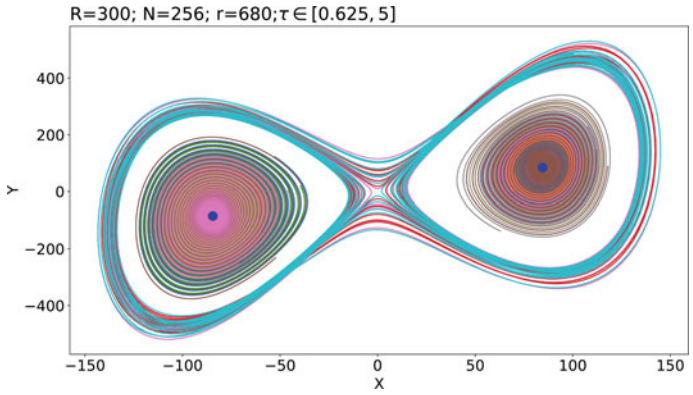

Fig. 4 Coexistence of chaotic and non-chaotic orbits starting with 256 different initial conditions (ICs) for $T \in [0.625, 5]$. Chaotic orbits recurrently return back to the saddle point at the origin. Non-chaotic orbits eventually approach one of two stable critical points as shown in large blue dots. Chaotic and non-chaotic orbits occupy different regions of attraction within the phase space

rate is proportional to the divergence of two nearby trajectories measured using a Lyapunov exponent. Within chaotic regimes of the 3DLM, as well as within the GLM that contains one positive LE and solution boundedness, time-varying divergence and convergence of nearby trajectories yields time-varying growth rates and, thus, time-varying predictability. Estimated predictability over a short period should display a dependence on various initial states.[9] By comparison, when non-chaotic (i.e., steady-state or nonlinear periodic) solutions appear as a single type of solution or coexist with another type of solution, their predictability should be deterministic (unlimited). Stated conservatively, the non-chaotic solution should remain predictable until it is changed by time varying parameters that represent heating or dissipations. As a result, very different intrinsic predictability may appear and depend on ICs within a system that possesses the coexistence of chaotic and non-chaotic attractors.

4 Attractor Coexistence Within the 3DLM

Within chaotic solutions of the 3DLM that has no stable equilibrium points, a tiny perturbation can always lead to a very different time evolution. Stated alternatively, within the chaotic regime, the system, in the absence of energy sinks for steady-state solutions, does not have a mechanism for completely removing the impact of a tiny perturbation on state variables. By comparison, within the GLM with M = 9, or higher, that possesses coexisting chaotic and steady-state solutions, a tiny initial perturbation may play a very different role. A tiny perturbation may have no

[9] As a result, we agree with Prof. Arakawa that the predictability limit is not necessarily a fixed value [46].

long-term impact when it appears to be associated with a steady-state solution that approaches one of the stable equilibrium points, suggesting that the perturbation eventually dissipates. On the other hand, a tiny perturbation may lead to a large impact on the time evolution of the chaotic solution. As a result, the 9DLM with a dual role for a tiny initial perturbation over a wide range of the heating parameter, as well as other features such as hierarchical scale dependence, is more realistic than the classical 3DLM with typical parameters. On the other hand, we may ask whether the 3DLM with different parameters may also produce two kinds of attractor coexistence, providing additional support to the findings of the GLM.

Next, we first discuss the coexistence of the 3DLM with typical parameters that include $\sigma = 10$. We then address the question of whether $\sigma = 10$ is a magic choice. As simply shown in the animation, https://goo.gl/scqRBo, the 3DLM with the same parameters, including r = 24.4, $\sigma = 10$, and b = 8/3, but with different ICs, produces two types of solutions that include chaotic or steady-state solutions, yielding the first kind of attractor coexistence. However, such a coexistence only appears over a very small range of r, giving the length of an interval less than 0.7 (i.e., $24.06 < r < r_c = 24.74$), and, thus, its characteristics and potential role in revealing the nature of weather has not been well appreciated.

For the past 50 years, although various types of solutions for Lorenz [6] have been documented, chaotic solutions have been the main focus. As discussed in the main text, since chaotic solutions appear over a finite range of parameters, their applicability in revealing the nature of weather depends on the realism of not only the models employed but also model parameter values. In his book in 1993, Lorenz humbly expressed that it may not have been possible for him to discover the butterfly-pattern solution if a realistic value of $\sigma = 1$ was used, as shown below:

> *I was lucky in more ways than one. An essential constant of the model is the Prandtl number – the ratio of the viscosity of the fluid to the thermal conductivity. Barry had chosen the value 10.0 as having the order of magnitude of the Prandtl number of water. As a meteorologist, he might well have chosen to model convection in air instead of water, in which case he would probably have used the value 1.0. With this value the solutions of the three equations would have been periodic, and I probably would never have seen any reason for extracting them from the original seven.*

Therefore, one may wonder how fortunate Prof. Lorenz was and whether a realistic value of $\sigma = 1$ may have influenced our view on the nature of weather. We make an attempt of addressing the question by analyzing a GLM with M = 9 and examining a 3DLM with $\sigma = 1$. As discussed in Shen [26], the GLM with M = 9 has stable, non-trivial equilibrium points for all $r > 1$ when $\sigma = 10$ and b = 8/3. To have stable, non-trivial equilibrium points for $\sigma = 1$ within the 3DLM, we chose b = 2/5. Such a choice leads to two kinds of attractor coexistence, a unique feature first identified within the 9DLM [26]. With $\sigma = 1$ in the 3DLM, the first kind of coexistence includes chaotic and steady-state solutions at a moderate heating parameter (e.g., r = 170, as shown in Fig. 5). Table 1 lists initial conditions for the results provided in Fig. 5. Thus, chaotic solutions may still appear within the 3DLM for a realistic value of $\sigma = 1$, but they coexist with steady-state solutions. The appearance of chaotic solutions depends not only on the range of the heating parameter but also on the

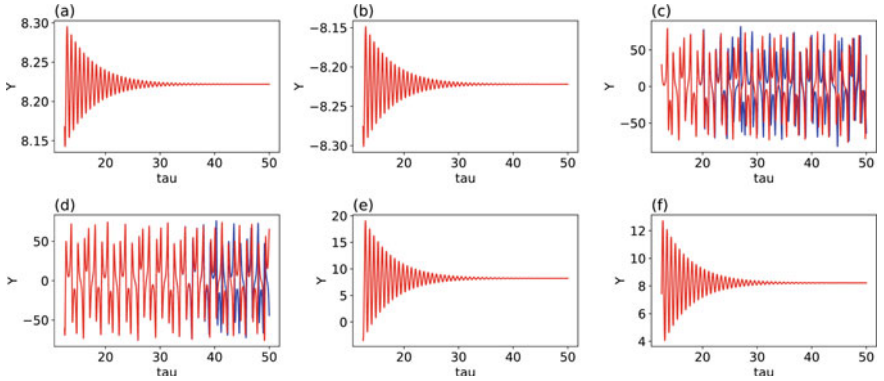

Fig. 5 A co-existence of chaotic (**c**, **d**) and non-chaotic (**a**, **b**, **e**, **f**) solutions using the same parameters for $\sigma = 1$, b = 0.4, and $r = 170$ within the 3DLM. Blue and red lines display solutions from the control and parallel runs, respectively. Initial conditions for the results in six panels are listed in Table 1

Table 1 Initial conditions (ICs) for revealing the coexistence of two attractors for $\sigma = 1$, $b = 0.4$, and $r = 170$ within the 3DLM. $X_c = Y_c = \sqrt{b(r-1)}$ and $Z_c = (r-1)$. The six rows provide the ICs for Fig. A1

X	Y	Z
X_c	$Y_c + 1$	Z_c
$-X_c$	$-Y_c + 1$	Z_c
0	1	0
−76.72346293	37.62433028	−146.96230812
−27.75526885	167.67883615	3.66782724
136.44623635	99.45689394	−19.76741851

ICs. Additionally, the second kind of coexistence that consists of a limit cycle and a steady-state solution appears at a large heating parameter (e.g., r = 250, not shown).

Both traditional and new model configurations with $(\sigma, b) = (10, 8/3)$ and $(1, 2/5)$, respectively, can produce chaotic solutions. For the traditional configuration that has been well applied in numerous studies since Lorenz [1], all three equilibrium points are unstable when $r > 24.74$. The stability of the three equilibrium points for $\sigma = 10$, as well as for $\sigma = 1$, is illustrated in Fig. 6. The non-existence of stable equilibrium points within the chaotic regime makes it easier to obtain chaotic solutions. However, no tiny, initial perturbation can completely lose its impact within the chaotic regime. We may interpret this as a finding that a tiny, initial perturbation cannot completely dissipate (before leading to a large impact). By comparison, for the new configuration of $\sigma = 1$, while the origin is still a saddle point, the two, non-trivial equilibrium points are stable (Fig. 6b). The existence of stable equilibrium points enables the coexistence of chaotic and steady-state solutions, the latter of which has no long-term memory regarding a tiny, initial perturbation.

As a result of coexistence for $\sigma = 1$ within the 3DLM, a proper choice of initial conditions is required in order to simulate a chaotic solution. Without knowing this,

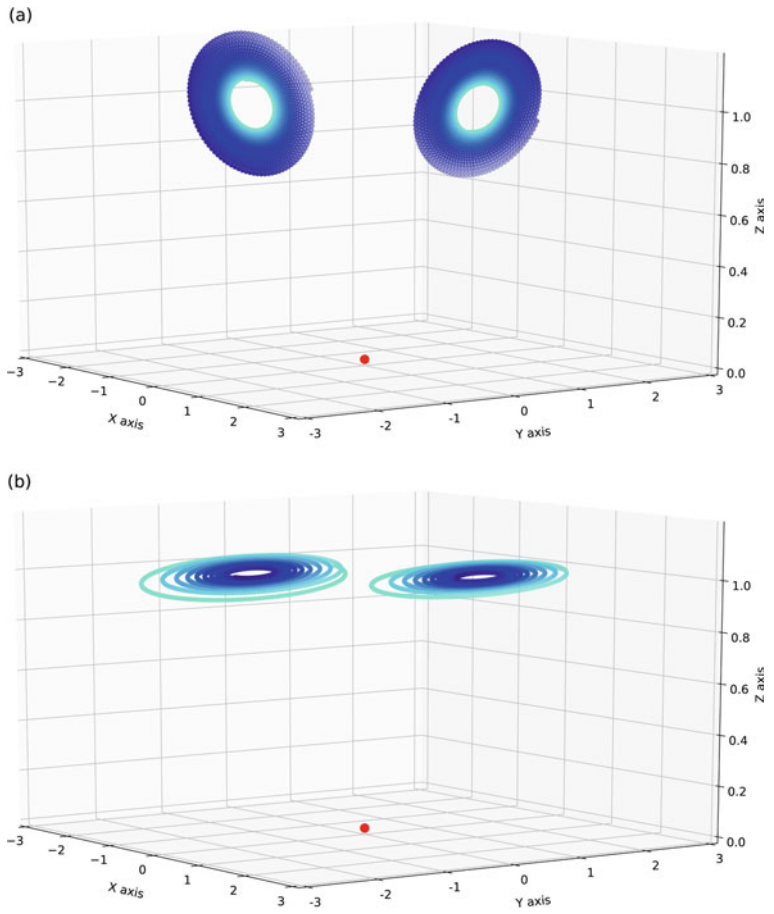

Fig. 6 Local behavior near the two non-trivial critical points for the 3DLM with $\sigma = 10$ (**a**) and $\sigma = 1$ (**b**). Lighter blue dots indicate the locations of orbits at earlier times. A red dot indicates the origin, which is a saddle point. Orbits in panel (**a**) spiral away from the non-trivial critical points while orbits in panel (**b**) spiral toward the non-trivial critical points

Prof. Lorenz thought it may have been impossible to obtain a "strange" solution if $\sigma = 1$ was first used in the Saltzman [30] model, giving no motivation for him to work on the 3DLM. In other words, the value of $\sigma = 10$ used in the original study [30] was indeed a "fortunate" choice so that an unexpected irregularly oscillatory solution could be revealed, inspiring Prof. Lorenz to develop the 3DLM in order to discover interesting chaotic features. However, on the other hand, we now understand that such a configuration can only depict a partial picture for the nature of weather. Based on our results and analysis, a realistic system should include physical processes for (some of) the tiny disturbances in order to completely dissipate. Since it produces the coexistence of chaotic and steady-state solutions and since the steady-state solution

has no long-term memory of tiny perturbations, the 3DLM with the new configuration of $\sigma = 1$ satisfies the objective. Such a system, which is similar to the 9DLM that produces two kinds of coexisting attractors, provides a more realistic view on the true nature of weather than the original 3DLM with a typical configuration. The above results support the idea that two kinds of attractor coexistence should be taken into consideration to reveal the nature of weather.

5 A Refined View on the Nature of Weather

Within the forced dissipative 3DLM, chaotic solutions appear within a finite range of parameters (e.g., heating parameter), bounded on one side by stable, steady-state solutions and on the other side by nonlinear periodic solutions. Since climate and weather involve open systems [60], an assumption of constant parameters within numerical simulations using the 3DLM, as well as high-dimensional LMs, is not realistic [61]. Time varying parameters that lead to different attractors should be used in models for realistic climate or weather [19]. For example, when a moderate heating becomes weaker (or stronger), a steady-state solution (or a limit cycle) may appear. Since regular and chaotic solutions may alternatively appear, chaotic solutions alone may not be able to represent the entirety of weather.

Additionally, our results show that chaotic and non-chaotic solutions may coexist and two kinds of attractor coexistence may alternatively appear within the 9DLM using time varying parameters. The analysis suggests a need to refine our view of weather by taking the dual nature associated with attractor coexistence into consideration. To this end, we suggest, contrary to the traditional view that weather is chaotic, that weather is, in fact, a superset that consists of both chaotic and non-chaotic processes, including both order and chaos.

5.1 Vacillation, Coexisting Two LCs, and Coexisting Two Time-Scale Orbits

The (potential) occurrence of a regular nonlinear periodic solution (i.e., limit cycle) in the atmosphere was first illustrated by laboratory experiments using dishpans. Based on experiments by Lorenz [39], Fultz [62] and Hide [63] suggested three types of solutions, including: (1) steady state solutions, (2) irregular chaotic solutions, and (3) vacillation. "Amplitude vacillation" is defined as a solution whose amplitude grows and periodically decays in a regular cycle [3, 64, 65]. Studies by Pedlosky [66], Smith [67], and Smith and Reilly [68] found that *amplitude vacillation can be viewed as a limit cycle solution.* By conducting a study for observational characteristics of

low-frequency variability, Ghil and Robertson [69] suggested that *40-day, intra-seasonal oscillations* may arise from a bifurcation off the blocking flow and *may be represented by a limit cycle with a period of 40 days.*

As discussed earlier, we showed that the 3DLM with a realistic value of $\sigma = 1$ also generates two kinds of attractor coexistence. Additionally, the coexistence of two stable limit cycle solutions was documented using the Lorenz 1984 model [15, 70–75] that also contains three types of solutions, including steady state, periodic solutions, and chaotic solutions. Using a seasonally varying forcing term with a time scale of 12 months, Lorenz [71] showed that chaos appears during winter (within a specific range of parameters) and two coexisting LCs during summer (within a different range of parameters). Such numerical results also support the view of the dual nature of chaos and order that alternatively appear. The above results suggest that once summer begins and has been observed, a better predictability for a limit cycle solution may be expected during each cycle of the solution in summer, as compared to that in winter. More recently, Lucarini and Bodai [76] applied a multistable system with coexisting attractors to reveal the bistability of the climate system with both positive and negative feedback [76, 77].

Coexisting solutions at two time scales, that are not the same as the coexisting attractors discussed above, have also been documented within the scientific literature. Related studies additionally support the refined view on the nature of weather. For example, co-existence of fast and slow manifolds has been discussed by Curry et al. [78], Lorenz [79, 80] and Lorenz and Krishnamurthy [81]. Both types of solutions in Lorenz [79] are non-chaotic. By comparison, fast and slow "variables" that are chaotic may also coexist within coupled systems [82, 83] In fact, an analysis using a singular perturbation method [84] indicates that the GLM also possesses the coexistence of slow and fast variables that correspond to large and very small spatial modes (e.g., Eqs. (2) and (4) of [27] in a high-dimension phase space). A current trend is to include time-varying parameters to increase the complexities of low order systems [85]. It can be shown that a higher dimensional Lorenz model (e.g., 7DLM) can be viewed as a lower-dimensional Lorenz model (e.g., 5DLM) with a periodic forcing, suggesting that the complexities of spatial mode–mode interaction may lead to the temporal complexities.

5.2 Error Saturations and Computational Chaos

In real-world weather models, the appearance of (fully) chaotic solutions may be indicated by error saturations, defined as follows. A logistic equation has been used to describe the evolution of root mean square (rms) average forecast error for ensemble runs [52, 86–89]. Given an initial condition with a small value, the solution of the logistic equation has time varying, non-negative growth rates (e.g., growing at an initial larger growth rate, then at a nonlinear smaller growth rate, and eventually approaching a constant defined as a saturated error that has a zero growth rate). The occurrence of error saturation at a fully nonlinear stage indicates a comparable

number of members with positive and negative error growth rates at a given time. Such a result is consistent with the features of a positive LE and solution boundedness associated with a specific chaotic solution.

The error growth model with non-negative growth rates may describe the statistical behavior of the system within which the majority of small errors tends to grow. *By comparison, the error growth model cannot accurately represent the initial, transient evolution of the rms averaged forecast error associated with large ensemble members with periodic or decaying components whose growth rates are small.* For periodic solutions such as vacillation [87], an ensemble averaged error may grow (or decay) with time when a large (or small) ensemble number of growing errors and a small (or large) ensemble number of decaying errors are averaged. As a result, when oscillatory waves were simulated, their rms errors may oscillate with time rather than become saturated. For example, oscillatory rms errors appeared after 40-day simulations in Fig. 5 of Liu et al. [90] who performed global simulations using the Community Atmosphere Model [91]. An additional example can be found in 30-day simulations of multiple African Easterly Waves (AEWs) using a global mesoscale model that produced oscillatory correlation coefficients [38].

On the other hand, it should be noted that error saturations may appear in association with computational chaos that is a numerical artifact. For example, Lorenz [92] presented several cases in order to show that while differential equations of a model may possess nonlinear limit cycle solutions, the corresponding discrete version of the model with large time steps produces a sensitive dependence of solutions on the initial condition, referred to as computational chaos. As a result, the appearance of error saturations (as well as positive LE) that appear within numerical models does not necessarily represent the chaotic nature of weather. *Due to the appearance of computational chaos, an estimate of a practical predictability limit using saturation errors should be interpreted with caution, as it does not necessarily represent an intrinsic predictability limit for real weather.*

6 Concluding Remarks

The statement of "weather is chaotic" has been introduced to indicate the chaotic nature of weather with a finite intrinsic predictability. The statement has also been cited to embrace a practical predictability limit of 2 weeks [93]. The finite intrinsic and practical predictability are indeed largely derived from the chaotic and unstable solutions of Lorenz models [1, 4]. In other words, the current view of "weather is chaotic" does not take into consideration other types of solutions within original Lorenz models and new types of solutions within newly developed generalized Lorenz models.

In this study, we first applied the aforementioned models in order to reveal three types of solutions and two kinds of attractor coexistence, indicating different intrinsic predictability for different solutions. We then suggested a refined view on the dual nature of chaos and order in weather. In contrast to the current view that

focuses on chaotic solutions with a predictability limit (of 2 weeks), our refined view suggests that coexisting chaotic and non-chaotic systems can have different intrinsic predictability. *The refined view may unify the theoretical understanding of different predictability within Lorenz models with recent numerical simulations of advanced global models that can simulate large-scale tropical waves beyond two weeks* [38, 94].

The refined view with a duality of chaos and order is fundamentally different from the Laplacian view of deterministic predictability and the Lorenz view of deterministic chaos. The refined view that is not too optimistic nor too pessimistic suggests both potential and challenges. For non-chaotic processes with steady-state or nonlinear periodic solutions [95, 96], their intrinsic predictability is deterministic (e.g., up to the lifetime of a dissipative solution or the time scale of the forcing) and their practical predictability can be continuously increased by improving the accuracy of the model and the initial conditions. For limit cycle solutions that may be associated with computational chaos, accurate simulations with better predictability, as compared to chaotic solutions, can be obtained by increasing temporal resolutions and/or removing redundant dissipations. To reveal longer predictability or better estimates on predictability in model and observation data, we will focus on developing schemes for the detection of chaotic and non-chaotic solutions [16, 28, 97] and examining the roles of butterfly effects in multiscale simulations using high-resolution global models.

In addition to the chaotic nature of weather with a finite predictability, another major influential impact of the 3DLM is that the sensitive dependence on initial condition, referred to as the butterfly effect of the first kind, has been inaccurately metaphorized to indicate the ability of a butterfly flap in creating a tornado [98], referred to as the butterfly effect of the second kind [7]. To understand their roles in reality and numerical models, the two different kinds of butterfly effects are being analyzed based on a comprehensive review of historical literature and recent understanding of chaos dynamics.

Acknowledgements We thank reviewers of the manuscript, the editor, and Drs. M. Alexander, R. Anthes, B. Bailey, J. Buchmann, D. Durran, M. Ghil, F. Judt, B. Mapes, Z. Musielak, T. Krishnamurti (Deceased), C.-D. Lin, T. Palmer, J. Pedlosky, J. Rosenfeld, R. Rotunno, I. A. Santos, C.-L. Shie, S. Vannitsem, and F. Zhang (Deceased) for valuable comments and discussions. We appreciate the eigenvalue analysis provided by Mr. N. Ferrante. We are grateful for support from the College of Science at San Diego State.

References

1. E.N. Lorenz, Deterministic nonperiodic flow. J. Atmos. Sci. **20**, 130–141 (1963)
2. E.N. Lorenz, Predictability: Does the flap of a butterfly's wings in Brazil set off a tornado in Texas? in *Proceedings of 139th Meeting of AAAS Section on Environmental Sciences, New Approaches to Global Weather: GARP* (Cambridge, MA, AAAS), 5 pp (1972). https://eaps4.mit.edu/research/Lorenz/Butterfly_1972.pdf

3. E.N. Lorenz, The mechanics of vacillation. J. Atmos. Sci. **20**, 448–464 (1963)
4. E.N. Lorenz, The predictability of a flow which possesses many scales of motion. Tellus **21**, 289–307 (1969)
5. J. Gleick, *Chaos: Making a New Science* (Penguin, New York, 1987), p. 360
6. E.N. Lorenz, The predictability of hydrodynamic flow. Trans. N.Y. Acad. Sci., Ser. II, **25**(4), 409–432 (1963)
7. B.-W. Shen, Nonlinear feedback in a five-dimensional Lorenz model. J. Atmos. Sci. **71**, 1701–1723 (2014). https://doi.org/10.1175/JAS-D-13-0223.1
8. S. Faghih-Naini, B.-W. Shen, Quasi-periodic in the five-dimensional non-dissipative Lorenz model: the role of the extended nonlinear feedback loop. Int. J. Bifurc. Chaos **28**(6) 1850072 (20 pages) (2018). https://doi.org/10.1142/S0218127418500724
9. C.C. Felicio, P.C. Rech, On the dynamics of five- and six-dimensional Lorenz models. J. Phys. Commun. **2**, 025028 (2018)
10. J. Guckenheimer, R.F. Williams, Structural stability of Lorenz attractors. Publ. Math. IHES. **50**, 59 (1979)
11. W.M. Macek, Nonlinear dynamics and complexity in the generalized Lorenz system. Nonlinear Dyn. **94**, 2957–2968 (2018). https://doi.org/10.1007/s11071-018-4536-z
12. S. Moon, B.-S. Han, J. Park, J.M. Seo, J.-J. Baik, Periodicity and chaos of high-order Lorenz systems. Int. J. Bifurc. Chaos **27**(11) 1750176 (11 pages) (2017). https://doi.org/10.1142/S0218127417501760.
13. S. Moon, J.M. Seo1, B.-S. Ha, J. Park, J.-J. Baik, A physically extended Lorenz system. Chaos **29**, 063129 (2019). https://doi.org/10.1063/1.5095466
14. Z.E. Musielak, D.E. Musielak, K.S. Kennamer, The onset of chaos in nonlinear dynamical systems determined with a new fractal technique. Fractals **13**, 19–31 (2005)
15. R.A. Pielke, X. Zeng, Long-term variability of climate. J. Atmos. Sci. **51**, 155–159 (1994)
16. T. Reyes, B.-W. Shen, A recurrence analysis of chaotic and non-chaotic solutions within a generalized nine-dimensional lorenz model. Chaos, Soliton. Fract. **125**(2019), 1–12 (2019). https://doi.org/10.1016/j.chaos.2019.05.003
17. D. Roy, Z.E. Musielak, Generalized Lorenz models and their routes to chaos. I. energy-conserving vertical mode truncations. Chaos Soliton. Fract. **32**, 1038–1052 (2007)
18. B.-W. Shen, Solitary waves, homoclinic orbits, and nonlinear oscillations within the non-dissipative Lorenz model, the inviscid pedlosky model, and the kdv equation, in *The 13th Chaos International Conference (CHAOS2020)*, 9–12 June 2020. https://doi.org/10.1007/978-3-030-70795-8_58 (in press)
19. B.-W. Shen, R.A. Pielke Sr., X. Zeng, J.-J. Baik, S. Faghih-Naini, J. Cui, R. Atlas, Is weather chaotic? Coexistence of chaos and order within a generalized Lorenz model. Bull. Am. Meteorol. Soc. 2021;102(1):E148–58. https://doi.org/10.1175/BAMS-D-19-0165.1
20. S. Smale, Mathematical problems for the next century. Math. Intell. **20**(2), 7–15 (1998)
21. C. Sparrow, *The Lorenz Equations: Bifurcations, Chaos, and Strange Attractor*. (Springer, New York, 1982). 269 pp. Appl. Math. Sci.
22. J.C. Sprott, X. Wang, G. Chen, Coexistence of point, periodic and strange attractors. Int. J. Bifurc. Chaos **23**(5) (2013). https://doi.org/10.1142/S0218127413500934
23. W. Tucker, A rigorous ODE Solver and Smale's 14th problem. Found. Comput. Math. **2**, 53–117 (2002)
24. Q. Yang, G. Chen, A chaotic system with one saddle and two stable node-foci. Int. J. Bifurc. Chaos **18**(5), 1393–1414 (2008)
25. T. Reyes, B.-W. Shen, A recurrence analysis of multiple African easterly waves during summer 2006, in *Current Topics in Tropical Cyclone Research, Anthony Lupo, IntechOpen*, 2020. https://doi.org/10.5772/intechopen.86859
26. B.-W. Shen, Aggregated negative feedback in a generalized Lorenz model. Int. J. Bifurc. Chaos **29**(3), 1950037 (2019). https://doi.org/10.1142/S0218127419500378
27. B.-W. Shen, T.A.L Reyes, S. Faghih-Naini, Coexistence of chaotic and non-chaotic orbits in a new nine-dimensional Lorenz model, in: C. Skiadas, I. Lubashevsky (Eds.) *11th Chaotic Modeling and Simulation International Conference. CHAOS 2018. Springer Proceedings in Complexity* (Springer, Cham). https://doi.org/10.1007/978-3-030-15297-0_22

28. J.C. Sprott, A. Xiong, Classifying and quantifying basins of attraction. Chaos **25**, 083101 (2015). https://doi.org/10.1063/1.4927643
29. J.C. Sprott, J.A. Vano, J.C. Wildenberg, M.B. Anderson, J.K. Noel, Coexistence and chaos in complex ecologies. Phys. Lett. A **335**(2005), 207–212 (2005)
30. B. Saltzman, Finite amplitude free convection as an initial value problem. J. Atmos. Sci. **19**, 329–341 (1962)
31. M. Hirsch, S. Smale, R.L. Devaney, *Differential Equations, Dynamical Systems, and an Introduction to Chaos*, 3rd edn. (Academic Press, 2013), 432 pp
32. J.M.T. Thompson, H.B. Stewart, *Nonlinear Dynamics and Chaos*, 2nd edn. (John Wiley & Sons, LTD, 2002), p. 437
33. P.G. Drazin, *Nonlinear Systems* (Cambridge), 333pp (1992)
34. J. Pedlosky, C. Frenzen, Chaotic and periodic behavior of finite-amplitude baroclinic waves. J. Atmos. Sci. **37**, 1177–1196 (1980)
35. J. Guckenheimer, P. Holmes, *Nonlinear Oscillations, Dynamical Systems, and Bifurcations of Vector Fields* (Springer, New York, 1983), p. 459
36. T. Shimizu, Analytical form of the simplest limit cycle in the Lorenz model. Physica **97A**, 383–398 (1979)
37. S.H. Strogatz, *Nonlinear Dynamics and Chaos. With Applications to Physics, Biology, Chemistry, and Engineering* (Westpress view, Boulder, CO, 2015), p. 513
38. B.-W. Shen, On the predictability of 30-day global mesoscale simulations of African easterly waves during summer 2006: a view with the generalized Lorenz model. Geosciences **9**, 281 (2019). https://doi.org/10.3390/geosciences9070281
39. E.N. Lorenz, *The Essence of Chaos* (University of Washington Press, Seattle, 1993), p. 227
40. E.N. Lorenz, *2008: The Butterfly Effect* (University of Rome, Rome, Premio Felice Pietro Chisesi e Caterina Tomassoni Award Lecture, April 2008).
41. B.-W. Shen, Hierarchical scale dependence associated with the extension of the nonlinear feedback loop in a seven-dimensional Lorenz model. Nonlin. Proces. Geophys. **23**, 189–203 (2016). https://doi.org/10.5194/npg-23-189-2016
42. A. Wolf, J.B. Swift, H.L. Swinney, J.A. Vastano, Determining Lyapunov exponents from a time series. Physica **16D**, 285–317 (1985)
43. X. Zeng, R. Eykholt, R.A. Pielke, Estimating the Lyapunov-exponent spectrum from short time series of low precision. Phys. Rev. Lett. **66**, 3229–3232 (1991)
44. X. Zeng, R.A. Pielke Sr., R. Eykholt, Chaos theory and its applications to the atmosphere. Bull. Atmos. Meteorol. Soc. **74**(4), 631–644 (1993)
45. R.C. Hilborn, *Chaos and Nonlinear Dynamics. An Introduction for Scientists and Engineers,* 2nd ed. (Oxford University Press, New York, 2000), pp. 650
46. B. Bailey, Quantifying the predictability of noisy space-time dynamical processes. Stat. Interf. **4**, 535–549 (2011)
47. R.O. Ding, J.P. Li, Nonlinear finite-time Lyapunov exponent and predictability. Phys. Lett. **354A**, 396–400 (2007)
48. B. Eckhardt, D. Yao, Local Lyapunov exponents in chaotic systems. Physica D **65**, 100–108 (1993)
49. J.M. Nese, Quantifying local predictability in phase space. Physica D. **35**, 237–250 (1989)
50. E. Ott, *Chaos in Dynamical Systems*, 2nd edn. (Cambridge University Press, 2002), 478pp
51. J. Yorke, E. Yorke, Metastable chaos: the transition to sustained chaotic behavior in the Lorenz model. J. Stat. Phys. **21**, 263–277 (1979)
52. E.N. Lorenz, Predictability—A problem partly solved. Seminar on Predictability, vol. I, ECMWF (1996) (also, published as Lorenz (2006))
53. E.N. Lorenz, Designing chaotic models. J. Atmos. Sci. **62**, 1574–1587 (2005)
54. E.N. Lorenz, Predictability – A problem partly solved, in T. Palmer, R. Hagedorn (eds.), *Predictability of Weather and Climate*). (Cambridge University Press, Cambridge, 2006), pp. 40–58. https://doi.org/10.1017/CBO9780511617652.004
55. J. Park, H. Lee, Y.-L. Jeon, J.-J. Baik, Periodicity of the Lorenz-Stenflo equations. Phys. Scr. **90**, 065201 (2015)

56. J. Park, B.-S. Han, H. Lee, Y.-L. Jeon, J.-J. Baik, Stability and periodicity of high-order Lorenz-Stenflo equations. Phys. Scr. **91**, 065202 (2016)
57. J.C. Xavier, P.C. Rech, Regular and chaotic dynamics of the Lorenz-Stenflo system. Int. J. Bifurc. Chaos **20**, 145–152 (2010)
58. Y. Saiki, E. Sander, J.A. Yorke, Generalized Lorenz equations on a three-sphere. Eur. Phys. J. Spec. Top. **226**, 1751–1764 (2017)
59. C. Grebogi, S.W. McDonald, E. Ott, J.A. Yorke, Final state sensitivity: an obstruction to predictability. Phys. Lett. A **99**(9), 415–418 (1983)
60. K. McGuffie, A. Henderson-Sellers, *The Climate Modeling Primer*, 4th edn. (John Wiley & Sons, Ltd, 2014), p. 439
61. J.D. Daron, D.A. Stainforth, 2015: On quantifying the climate of the nonautonomous Lorenz-63 model. Chaos **25**, 043103 (2015). https://doi.org/10.1063/1.4916789
62. D. Fultz, R.R. Long, G.V. Owens, W. Bohan, R. Kaylor, J. Weil, Studies of thermal convection in a rotating cylinder with some implications for large-scale atmospheric motion. Meteorol. Monographs **21**(4) (1959). (American Meteorological Society)
63. R. Hide, Some experiments on thermal convection in a rotating liquid. Quart. f. Roy. Meteorol. Soc. **79**, 161 (1953)
64. M. Ghil, P. Read, L. Smith, 2010: Geophysical flows as dynamical systems: the influence of Hide's experiments. Astron. Geophys. **51**(4), 428–435 (Aug. 2010). https://doi.org/10.1111/j.1468-4004.2010.51428.x
65. M. Ghil, S. Childress, *Topics in Geophysical Fluid Dynamics: Atmospheric Dynamics, Dynamo Theory, and Climate Dynamics* (Springer, New York, 1987), p. 485
66. J. Pedlosky, Limit cycles and unstable baroclinic waves. J. Atmos. Sci. **29**, 53–63 (1972)
67. R.K. Smith, A note on a theory of vacillating baroclinic waves. J. Atmos. Sci. **32**, 2027 (1975)
68. R.K. Smith, J.M. Reilly, On a theory of amplitude vacillation in baroclinic waves: some numerical solutions. J. Atmos. Sci. **34**, 1256–1260 (1977)
69. M. Ghil, A.W. Robertson, "Waves" vs. "particles" in the atmosphere's phase space: a pathway to long-range forecasting? PNAS **99**(suppl 1) 2493–2500 (2002). https://doi.org/10.1073/pnas.012580899
70. E.N. Lorenz, Irregularity: a fundamental property of the atmosphere, in *Crafoord Prize Lecture, presented at the Royal Swedish Academy of Sciences, Stockholm, September 28, 1983*. Tellus, 36A, 98–110 (1984) (LM84)
71. E.N. Lorenz, Can chaos and intransitivity lead to interannual variability? Tellus **42A**, 378–389 (1990)
72. C. Masoller, A.C. Sicardi Schifino, L. Romanelli, Regular and chaotic behavior in the new Lorenz system. Phys. Lett. A **167**(1992), 185–190 (1992)
73. L. Veen van, Time scale interaction in low-order climate models. Utrecht University Repository. (PhD Dissertation) (2002)
74. L. Veen, Baroclinic flow and the Lorenz-84 mode. Int. J. Bifurc. Chaos **13**, 2117 (2003). https://doi.org/10.1142/S0218127403007904
75. H. Wang, Y. Yu, G. Wen, Dynamical analysis of the Lorenz-84 atmospheric circulation model. J. Appl. Math. **2014**, 296279, 15 pp (2014). https://doi.org/10.1155/2014/296279
76. V. Lucarini, T. Bodai, 2019: Transitions across melancholia states in a climate model: reconciling the deterministic and stochastic points of view. Phys. Rev. Lett. **122**, 158701 (2019)
77. I.R. Garashchuk, D.I. Sinelshchikov, A.O. Kazakov, N.A. Kudryashov, Hyperchaos and multistability in the model of two interacting microbubble contrast agents editors-pick. Chaos **29**, 063131 (2019). https://doi.org/10.1063/1.5098329
78. J.H. Curry, S.E. Haupt, M.N. Limber, Truncated systems, initialization, and the slow manifold. Tellus **47A**, 145161 (1995)
79. E.N. Lorenz, On the existence of a slow manifold. J. Atmos. Sci. **43**, 154471557 (1986)
80. E.N. Lorenz, The slow manifold. What is it? J. Atmos. Sci. **49**, 24492451 (1992)
81. E.N. Lorenz, V. Krishnamurthy, On the nonexistence of a slow manifold. J. Atmos. Sci. **44**, 29402950 (1987)

82. L. Mitchell, G.A. Gottwald, Data assimilation in slow-fast systems using homogenized climate models. J. Atmos. Sci. **69**, 1359–1377 (2012). https://doi.org/10.1175/JAS-D-11-0145.1
83. M. Peña, E. Kalnay, 2004: Separating fast and slow modes in coupled chaotic systems. Nonlin. Proces. Geophys. **11**, 319–327 (2004). https://doi.org/10.5194/npg-11-319-2004
84. C.M. Bender, S.A. Orszag, *Advanced Mathematical Methods for Scientists and Engineers* (McGraw-Hill, New York, 1978), p. 593
85. V. Lucarini, Stochastic resonance for nonequilibrium systems. Phys. Rev. E **100**, 062124 (2019). https://doi.org/10.1103/PhysRevE.100.062124
86. E. Kalnay, *Atmospheric Modeling, Data Assimilation and Predictability* (Cambridge, New York, 2003), 369 pp
87. E.N. Lorenz, Atmospheric predictability as revealed by naturally occurring analogues. J. Atmos. Sci. **26**, 636–646 (1969)
88. C. Nicolis, 1992: Probabilistic aspects of error growth in atmospheric dynamics. Q. J. R. Meteorol. Soc. **118**, 553–568 (1992)
89. F. Zhang, Y.Q. Sun, L. Magnusson, R. Buizza, S.-J. Lin, J.-H. Chen, K. Emanuel, What Is the predictability limit of midlatitude weather? J. of Atmos. **76**, 1077–1091 (2019)
90. H.-L. Liu, F. Sassi, R.R. Garcia, Error growth in a whole atmosphere climate model. J. Atmos. Sci. **66**, 173–186 (2009)
91. W.D. Collin et al., Description of the NCAR Community Atmosphere Model (CAM3). NCAR Tech. Note NCAR/TN-464+STR, 226pp (2004)
92. E.N. Lorenz, Computational chaos: a prelude to computational instability. Physica **35D**, 299–317 (1989)
93. Lewis, Roots of ensemble forecasting. Mon. Weather Rev. **133**(7), 1865–1885 (2005)
94. F. Judt, Atmospheric predictability of the tropics, middle latitudes, and polar regions explored through global storm-resolving simulations. J. Atmos. Sci. **77**, 257–276 (2020). https://doi.org/10.1175/JAS-D-19-0116.1
95. B.-W. Shen, Homoclinic orbits and solitary waves within the non-dissipative Lorenz model and KdV equation. Int. J. Bifurc. Chaos. **30**, 2050257–1–2050315 (2020). https://doi.org/10.1142/S0218127420502570
96. B.-W. Shen, On periodic solutions in the non-dissipative Lorenz model: the role of the nonlinear feedback loop. Tellus A **70**, 1471912 (2018). https://doi.org/10.1080/16000870.2018.1471912
97. J. Cui, B.-W. Shen, A Kernel Principal Component Analysis of Coexisting Attractors within a Generalized Lorenz Model. Chaos, Solitons & Fractals, 146. https://doi.org/10.1016/j.chaos.2021.110865
98. R. Pielke, The real butterfly effect (2008). https://pielkeclimatesci.wordpress.com/2008/04/29/the-realbutterfly-effect/